ISSN 0915-633X

NATIONAL INSTITUTE FOR FUSION SCIENCE

New High Voltage Parallel Plate Analyzer

Y. Hamada, Y. Kawasumi, K. Masai, H. Iguchi,
A. Fujisawa, JIPPT-11U Group and Y. Abe

(Received – Nov. 28, 1991)

NIFS-128 Jan. 1992

RESEARCH REPORT
NIFS Series

NAGOYA, JAPAN

New High Voltage Parallel Plate Analyzer

Y. Hamada, Y. Kawasumi, K. Masai, H. Iguchi,
A. Fujisawa, and JIPPT-11U group

National Institute for Fusion Science
Nagoya, 464-01, Japan

Y. Abe,

Faculty of Engineering, Iwate University,
Morioka, Iwate, 020, Japan

ABSTRACT. A new modification on the parallel plate analyzer for 500keV heavy ions to eliminate the effect of the intense UV and visible radiations, is successfully conducted. Its principle and results are discussed.

$1 Introduction

The parallel plate electrostatic energy analyzer[1,2] is widely used in various fields of experimental physics and technology because of its simplicity and good focusing properties up to the second order. The practical setup of the analyzer usually consists of the simple upper and lower electrodes and a few number of guard rings with resister chains in order to improve the uniformity of the electric field between the plates.[1,2] In the case of analyzing 100keV to MeV particles, the suppression of electrical breakdown of the electrode and the heat removal of the resistors in the guard ring are key issues. Recently in the experiment of the high temperature plasma physics, the gold, cesium or thallium beams with the energy of 100keV to MeV are injected into the magnetically confined plasmas in order to measure the local plasma potentials and turbulence(Heavy Ion Beam Probe)[3-4]. The change of the energy of the secondary beam generated in the plasma, corresponds to the local plasma potentials where the ionization takes place.[5] For the measurement of this energy change, the electric energy analyzer can be more compact compared to the magnetic analyzer, if we are able to suppress the electric breakdown, since the required dimension of the electric analyzer is independent of the mass number of the particles.

The energy analyzer in the high temperature plasma is, however, irradiated by the very intense visible, UV, VUV and soft x-ray lights emitted by the plasma. The intense light in the energy analyzer induces the secondary electron emissions in the analyzer. Some of the electrons flow into the guard ring of the parallel plate analyzer. The electron flow in the resistor train of the guard rings changes the electric field inside the analyzer and induces the error in the measurement. In order to reduce this change to an acceptable level, the resistance of the resistors placed between the rings, should be small. The reduction of the resistance of the resistors on the high voltage plate in the vacuum, however, results in the large heat consumption and causes serious problems. The resistors of the analyzer of HIBP(0.5 MeV, thallium beam) in TEXT tokamak are removed out of the vacuum vessel and are cooled in the oil bath[3]

Another method to improve the uniformity of the electric field and to suppress the electrical breakdown between the parallel plates, may be the adoption of the shaped electrodes, as was suggested by TEXT HIBP group.[3] The numerical optimization of the shaped electrodes and the first experimental results of the new energy analyzer of this type, to our knowledge, for the 500keV HIBP in JIPPT-IIU tokamak[6], are discussed in this paper.

§2 Analyzer model and theory

Figure 1a and b show the cross-sectional and side views of our simplified model of parallel plate analyzer. Vacuum vessel itself serves as the outer boundary of the zero potential and the lower electrode. The circular ring is attached to the upper electrode in order to increase the region of uniform electric field, which also serves as the corona ring to suppress the breakdown of the high voltage of about 100kV. The optimal radius of the ring is determined numerically by the 2-dimensional boundary element method[7]. Results of the optimization are given in Table 1 and the potential distributions in the optimized case are shown in Figure 3. The optimized radius(Ac) of the corona ring normalized by the distance(H1) between upper and lower electrodes, is Ac = 0.168, while the normalized radius(Av) of the vacuum vessel and the width of upper electrode(2 X S1), are selected to be 2.5 and 3.0 respectively. As is shown in Table 1, the deviation from the linearity of the potential on the y axis(symmetry axis in Figure 1a) is reduced to less than 10^{-4} by the optimization. The region of the uniform electric field may not be so wide at higher position (h=0.75, for example), as is shown in Figure 3, because of the single optimization parameter of Ac. The height in the trajectory of the ion is, however, confined below h=0.633 in the design.

The trajectory of the particle in the exit field-free region is written by the simple equation,

$$x = (h_i + h_d)\cot\theta + 2.0\mathrm{H1}\frac{V_b}{Q_b V_a}\sin 2\theta \quad , \qquad (1)$$

where θ, is the entrance angle in the plane of the analyzer. V_a is the voltage of the upper electrode. Q_b, and V_b are the charge number and the energy of the beam in the units of electron volt. Other quantities are shown in figure 2. By the focusing condition,

$$\partial x / \partial\theta = 0 \quad ,$$

we can have the focusing distance,

$$x = H1 \frac{2.0V_b}{Q_b V_a} \sin 2\theta (\cos 2\theta + 1) \quad (2)$$

At θ = 30 degrees, it has the second order focus in the injection angle,

$$\partial^2 x / \partial^2 \theta = 0,$$

and the longest focus distance(L1),

$$L1 = \frac{3\sqrt{3}}{2} H1 \frac{V_b}{Q_b V_a}. \quad (3)$$

The characteristics of the analyzer are conveniently described by the gain function $G(\theta,\varphi)$, the ratio of the beam voltage to the analyzer voltage,

$$G(\theta,\varphi) = V_b / V_a, \quad (4)$$

where φ is the entrance angle perpendicular to the plane of analyzer. The gain function is dependent on the beam position and can be obtained by modifying equation (1),

$$G(\theta,\varphi) = \frac{Q_b}{2H1} \frac{(L1 + d\cos\theta_o) - (h_i + h_d + d\cos\theta_o)\cot\theta}{\sin 2\theta \cos^2 \varphi}, \quad (5)$$

where the detector is slid along the angle of θ_0 from the position of the second-order focus, with the distance of d. Figure 4 shows the theoretical gain curves as a function of the in-plane entrance angle θ, in the case of φ = 0.0 and θ_0 = 30 degrees, as a parameter of the length(δ) of the slid motion of detectors normalized by the distance between the input slit and the theoretical focus point(L1). It clearly shows that the first-order focus point approaches together as the deviation from the second-focus point gets smaller and at δ=0, the second-order focus is obtained at the injection angle of 30 degrees. The condition that the trajectory of the beam must be confined below the upper electrode, is expressed by

$$G(\theta) \le Q_b / \sin^2\theta. \qquad (6)$$

The gain must be smaller than 8 for doubly ionized beam for 30 degrees injection angle.

§3 Experimental Results

The selected gain for doubly ionized particles is 5.0 under the condition that the voltage of the upper electrode should not exceed 100kV for the 0.5MeV beam detection from the plasma and the beam should not reach the region where the uniformity of the electric field at higher position(h =0.75 in Figure 3, for example) is somewhat degraded because of the only one optimization parameter of Ac. As for the physical dimension, the distance between the electrodes(H1) is 10cm and the total length of the vacuum vessel is about 1m.

For the tuning of the entrance angles (in-plane and out-of-plane of analyzer) to 30 and 0 degrees, the whole vacuum vessel can be tilted in two dimensional directions. The detector consists of simple four plates to measure the shift of the beam in two directions, mounted on the precision slide mount, 30 degrees to the parallel plate analyzer. Sliding of the detector of pair plates, along the 30 degrees slope, is very useful both for the precise measurement of the in-plane and out-of-plane entrance angles of the beam and for tuning the detector position to the focus point.

In Figure 4, the experimentally obtained values of analyzer gains are shown in contrast to the theoretically predicted curves of gains. Open and solid circles are the gains, when the 350keV Thallium ion beam is injected into JIPPT-11U tokamak and the Tl^{2+} beam generated in the plasma is detected by this analyzer. The experimental gains are normalized to the theoretical value of 5.0 at the injection angle of 30 degrees. The experimental data show that the focus point is shifted by about 5 percents from the theoretical position. The general trends, however, show the reasonable agreement with the design curve. It is found that the shift of the focus point is due to the defocusing effect of the rectangular slit holes placed on the lower electrode for the beam penetration, since the shift is greatly reduced in the case of fine mesh. The similar effect is predicted theoretically in the analysis of the effect of the slit placed on the inner electrode of a cylindrical mirror analyzer.[8] When we use the fine mesh, the effect of the beam deflection by the very local field near the lines of the mesh, is observed clearly on the pair plates of the detector and will cause the error in the measurement. The detailed discussion on the effect of the slit on the electrode in the parallel plate analyzer will be given in a separate paper.

Because of the intense stray light from the plasma, the current of about 1mA flows from the upper electrode to the boundary. But the high voltage power supply is highly stabilized and its effect is smaller by many orders than the error due to the change of the injection angle. The error due to the change of the injection angle is less than 0.1 percent when the in-plane injection angle is within plus and minus two degrees from 30 degrees.

In conclusion the simple shaped upper electrode and outer boundary of the vacuum vessel is employed in the high voltage parallel plate electrostatic energy analyzer irradiated by the intense UV light. It is found that the focus point is dependent on the separation of the wires of the mesh on the slit of the electrode. The analyzer characteristics, however, are found to be in reasonable agreement to the theoretical estimate and are free from the error due to the photo-current flowing into the guard resistors.

We would like to thank Professors, R. L. Hickok and K. A. Connor of Rensselaer Polytechnic Institute for their kind guidance and suggestion of this problem. In addition, the authors acknowledge Director A. Iiyoshi and Professor M. Fujiwara for their continuous supports.

Reference

1) G. A. Harrower, Rev. Sci. Instrum. **26,** 850(1855).
2) T. S. Green and G. A. Proca, Rev. Sci. Instrum. **41,** 1409(1970).
3) P. M. Schoch, A. Camevali, K. A. Conner, T. P. Crowley, J. C. Forster, R. L. Hickok, J. F.Lewis, and J. G. Schatz Jr, Rev. Sci. Instrum. **59(8),** 1646 (1988)
4) G. A. Hallock, J. Mathew, W. C. Jennings, and R. L. Hickok, Phys. Rev. Lett, **56** 1248(1986).
5) J. C. Jobes, and R. L. Hickok, Nuclear Fusion **10** 195 (1970)
6) K. Toi, Y. Hamada. et al., in Plasma Physics and Conrolled Nuclear Fusion Research 1990, Vol1, 301, IAEA, Vienna (1991).
7) C. A. Brebbia, The Boundary Element Method for Engineers Pentech Press, London(1978).
8) L. Frank, J. Phys. E: Sci. Instrum **9,** 670(1876).

Figure Captions

Figure 1

Schematics of the parallel plate analyzer, 1a) Cross-sectional view of the analyzer, 1b) side view.

Figure 2

Beam trajectory in the parallel plate energy analyzer.

Figure 3.

The potential distributions at various heights(h) in optimized case(Ac=0.168) and non-optimized case(Ac=0.05). The continuous and dashed lines correspond to Ac = 0.168

and Ac = 0.05, respectively. All distances are normalized by the height of the upper electrode(H1).

Figure 4

The theoretical gain functions(dashed lines) and the experimental data(circles). δ is the shift of the detector from the theoretical focus point, along the slope 30 degrees to the parallel plate, normalized by the total distance between the input slit and theoretical focus point(L1). In this case L1 = 64.. The experimental data are open(δ = 5.4%) and solid(δ = 2.7%) circles.

Table 1

Potentials at the various height(h) on the symmetry axis(x=0 in Figure 1a and 3), in the case of optimized radius of coronal ring(Ac=0.168) and in non-optimized case(Ac=0.05). The potential of the upper electrode is assumed to be 5 volt. Other parameters of the analyzer are not sensitive and fixed at values shown in the table.

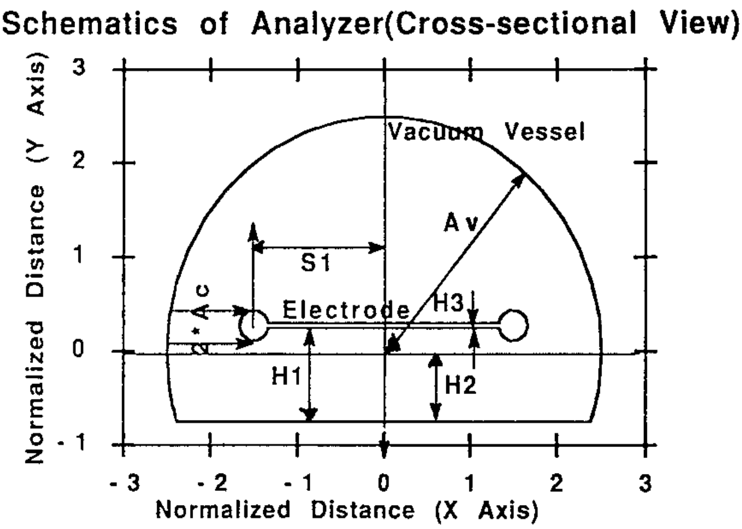

Figure 1a

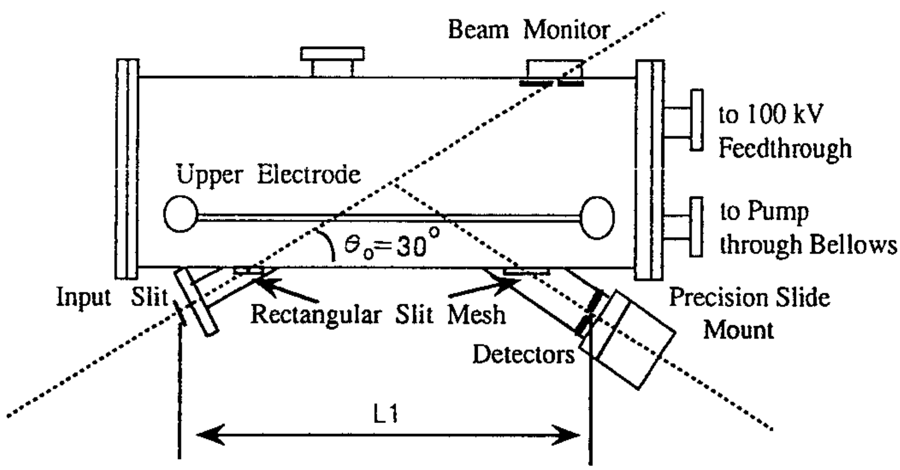

Figure 1b

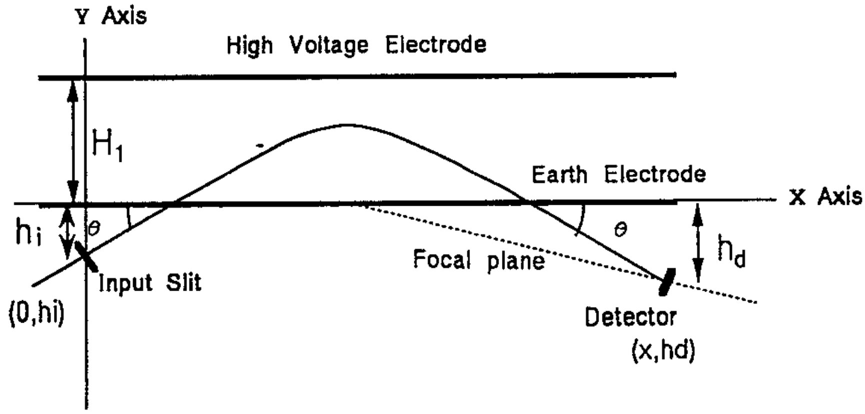

Figure 2

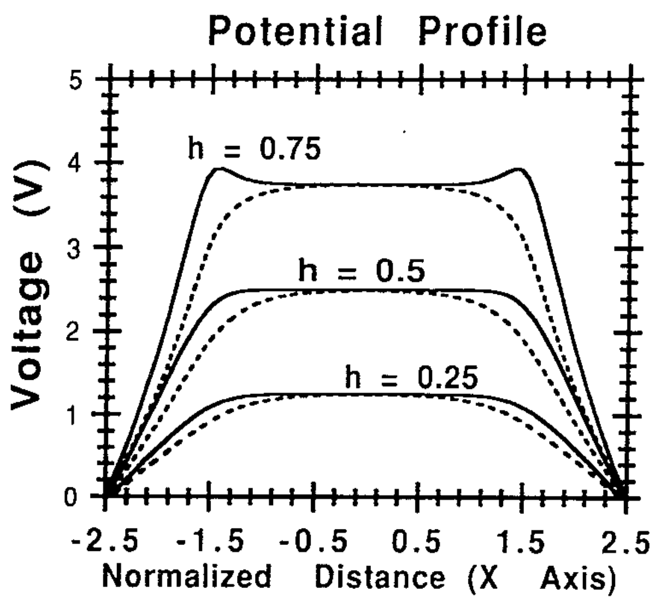

Figure 3

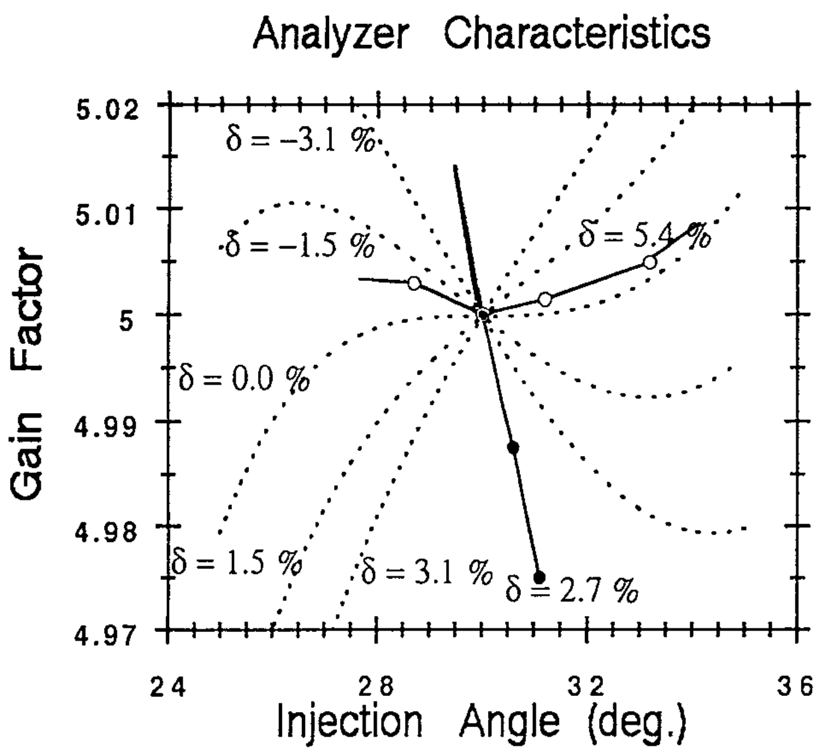

Figure 4

Ac \ h	1.0000	0.7500	0.5000	0.2500	0.0
0.1675	5.0000	3.7501	2.5000	1.2500	0.0
0.0500	5.0000	3.7416	2.4882	1.2404	0.0

Av=2.5, S1=1.5, H1=1.0, H2=0.75, H3=0.05

Table 1

Recent Issues of NIFS Series

NIFS-69 T.Kato, K.Masai, T.Fujimoto,F.Koike, E.Källne, E.S.Marmar and J.E.Rice,*He-like Spectra Through Charge Exchange Processes in Tokamak Plasmas;* Jan.1991

NIFS-70 K. Ida, H. Yamada, H. Iguchi, K. Itoh and CHS Group, *Observation of Parallel Viscosity in the CHS Heliotron/Torsatron* ; Jan.1991

NIFS-71 H. Kaneko, *Spectral Analysis of the Heliotron Field with the Toroidal Harmonic Function in a Study of the Structure of Built-in Divertor* ; Jan. 1991

NIFS-72 S. -I. Itoh, H. Sanuki and K. Itoh, *Effect of Electric Field Inhomogeneities on Drift Wave Instabilities and Anomalous Transport* ; Jan. 1991

NIFS-73 Y.Nomura, Yoshi.H.Ichikawa and W.Horton, *Stabilities of Regular Motion in the Relativistic Standard Map*; Feb. 1991

NIFS-74 T.Yamagishi, *Electrostatic Drift Mode in Toroidal Plasma with Minority Energetic Particles,* Feb. 1991

NIFS-75 T.Yamagishi, *Effect of Energetic Particle Distribution on Bounce Resonance Excitation of the Ideal Ballooning Mode*, Feb. 1991

NIFS-76 T.Hayashi, A.Tadei, N.Ohyabu and T.Sato, *Suppression of Magnetic Surface Breading by Simple Extra Coils in Finite Beta Equilibrium of Helical System;* Feb. 1991

NIFS-77 N. Ohyabu, *High Temperature Divertor Plasma Operation*; Feb. 1991

NIFS-78 K.Kusano, T. Tamano and T. Sato, *Simulation Study of Toroidal Phase-Locking Mechanism in Reversed-Field Pinch Plasma*; Feb. 1991

NIFS-79 K. Nagasaki, K. Itoh and S. -I. Itoh, *Model of Divertor Biasing and Control of Scrape-off Layer and Divertor Plasmas*; Feb. 1991

NIFS-80 K. Nagasaki and K. Itoh, *Decay Process of a Magnetic Island by Forced Reconnection*; Mar. 1991

NIFS-81 K. Takahata, N. Yanagi, T. Mito, J. Yamamoto, O.Motojima and LHDDesign Group, K. Nakamoto, S. Mizukami, K. Kitamura, Y. Wachi, H. Shinohara, K. Yamamoto, M. Shibui, T. Uchida and K. Nakayama, *Design and Fabrication of Forced-Flow Coils as R&D Program for Large Helical Device*; Mar. 1991

NIFS-82 T. Aoki and T. Yabe, *Multi-dimensional Cubic Interpolation for ICF Hydrodynamics Simulation*; Apr. 1991

NIFS-83 K. Ida, S.-I. Itoh, K. Itoh, S. Hidekuma, Y. Miura, H. Kawashima, M. Mori, T. Matsuda, N. Suzuki, H. Tamai, T.Yamauchi and JFT-2M Group, *Density Peaking in the JFT-2M Tokamak Plasma with Counter Neutral Beam Injection* ; May 1991

NIFS-84 A. Iiyoshi, *Development of the Stellarator/Heliotron Research*; May 1991

NIFS-85 Y. Okabe, M. Sasao, H. Yamaoka, M. Wada and J. Fujita, *Dependence of Au^- Production upon the Target Work Function in a Plasma-Sputter-Type Negative Ion Source;* May 1991

NIFS-86 N. Nakajima and M. Okamoto, *Geometrical Effects of the Magnetic Field on the Neoclassical Flow, Current and Rotation in General Toroidal Systems*; May 1991

NIFS-87 S. -I. Itoh, K. Itoh, A. Fukuyama, Y. Miura and JFT-2M Group, *ELMy-H mode as Limit Cycle and Chaotic Oscillations in Tokamak Plasmas;* May 1991

NIFS-88 N.Matsunami and K.Kitoh, *High Resolution Spectroscopy of H^+ Energy Loss in Thin Carbon Film;* May 1991

NIFS-89 H. Sugama, N. Nakajima and M.Wakatani, *Nonlinear Behavior of Multiple-Helicity Resistive Interchange Modes near Marginally Stable States;* May 1991

NIFS-90 H. Hojo and T.Hatori, *Radial Transport Induced by Rotating RF Fields and Breakdown of Intrinsic Ambipolarity in a Magnetic Mirror*; May 1991

NIFS-91 M. Tanaka, S. Murakami, H. Takamaru and T.Sato, *Macroscale Implicit, Electromagnetic Particle Simulation of Inhomogeneous and Magnetized Plasmas in Multi-Dimensions;* May 1991

NIFS-92 S. - I. Itoh, *H-mode Physics, -Experimental Observations and Model Theories-, Lecture Notes, Spring College on Plasma Physics, May 27 - June 21 1991 at International Centre for Theoretical Physics (IAEA UNESCO) Trieste, Italy ;* Jun. 1991

NIFS-93 Y. Miura, K. Itoh, S. - I. Itoh, T. Takizuka, H. Tamai, T. Matsuda, N. Suzuki, M. Mori, H. Maeda and O. Kardaun, *Geometric Dependence of the Scaling Law on the Energy Confinement Time in H-mode Discharges;* Jun. 1991

NIFS-94 H. Sanuki, K. Itoh, K. Ida and S. - I. Itoh, *On Radial Electric Field Structure in CHS Torsatron / Heliotron;* Jun. 1991

NIFS-95 K. Itoh, H. Sanuki and S. - I. Itoh, *Influence of Fast Ion Loss on Radial Electric Field in Wendelstein VII-A Stellarator;* Jun. 1991

NIFS-96 S. - I. Itoh, K. Itoh, A. Fukuyama, *ELMy-H mode as Limit Cycle and Chaotic Oscillations in Tokamak Plasmas;* Jun. 1991

NIFS-97 K. Itoh, S. - I. Itoh, H. Sanuki, A. Fukuyama, *An H-mode-Like Bifurcation in Core Plasma of Stellarators;* Jun. 1991

NIFS-98 H. Hojo, T. Watanabe, M. Inutake, M. Ichimura and S. Miyoshi, *Axial Pressure Profile Effects on Flute Interchange Stability in the Tandem Mirror GAMMA 10;* Jun. 1991

NIFS-99 A. Usadi, A. Kageyama, K. Watanabe and T. Sato, *A Global Simulation of the Magnetosphere with a Long Tail : Southward and Northward IMF;* Jun. 1991

NIFS-100 H. Hojo, T. Ogawa and M. Kono, *Fluid Description of Ponderomotive Force Compatible with the Kinetic One in a Warm Plasma* ; July 1991

NIFS-101 H. Momota, A. Ishida, Y. Kohzaki, G. H. Miley, S. Ohi, M. Ohnishi K. Yoshikawa, K. Sato, L. C. Steinhauer, Y. Tomita and M. Tuszewski *Conceptual Design of D-^{3}He FRC Reactor "ARTEMIS"* ; July 1991

NIFS-102 N. Nakajima and M. Okamoto, *Rotations of Bulk Ions and Impurities in Non-Axisymmetric Toroidal Systems* ; July 1991

NIFS-103 A. J. Lichtenberg, K. Itoh, S. - I. Itoh and A. Fukuyama, *The Role of Stochasticity in Sawtooth Oscillation* ; Aug. 1991

NIFS-104 K. Yamazaki and T. Amano, *Plasma Transport Simulation Modeling for Helical Confinement Systems;* Aug. 1991

NIFS-105 T. Sato, T. Hayashi, K. Watanabe, R. Horiuchi, M. Tanaka, N. Sawairi and K. Kusano, *Role of Compressibility on Driven Magnetic Reconnection ;* Aug. 1991

NIFS-106 Qian Wen - Jia, Duan Yun - Bo, Wang Rong - Long and H. Narumi, *Electron Impact Excitation of Positive Ions - Partial Wave Approach in Coulomb - Eikonal Approximation* ; Sep. 1991

NIFS-107 S. Murakami and T. Sato, *Macroscale Particle Simulation of Externally Driven Magnetic Reconnection;* Sep. 1991

NIFS-108 Y. Ogawa, T. Amano, N. Nakajima, Y. Ohyabu, K. Yamazaki, S. P. Hirshman, W. I. van Rij and K. C. Shaing, *Neoclassical Transport Analysis in the Banana Regime on Large Helical Device (LHD) with the DKES Code;* Sep. 1991

NIFS-109 Y. Kondoh, *Thought Analysis on Relaxation and General Principle to Find Relaxed State;* Sep. 1991

NIFS-110 H. Yamada, K. Ida, H. Iguchi, K. Hanatani, S. Morita, O. Kaneko, H. C. Howe, S. P. Hirshman, D. K. Lee, H. Arimoto, M. Hosokawa, H. Idei, S. Kubo, K. Matsuoka, K. Nishimura, S. Okamura, Y. Takeiri, Y. Takita and C. Takahashi, *Shafranov Shift in Low-Aspect-Ratio Heliotron / Torsatron CHS* ; Sep 1991

NIFS-111 R. Horiuchi, M. Uchida and T. Sato, *Simulation Study of Stepwise Relaxation in a Spheromak Plasma ;* Oct. 1991

NIFS-112 M. Sasao, Y. Okabe, A. Fujisawa, H. Iguchi, J. Fujita, H. Yamaoka and M. Wada, *Development of Negative Heavy Ion Sources for Plasma Potential Measurement* ; Oct. 1991

NIFS-113 S. Kawata and H. Nakashima, *Tritium Content of a DT Pellet in Inertial Confinement Fusion* ; Oct. 1991

NIFS-114 M. Okamoto, N. Nakajima and H. Sugama, *Plasma Parameter Estimations for the Large Helical Device Based on the Gyro-Reduced Bohm Scaling* ; Oct. 1991

NIFS-115 Y. Okabe, *Study of* Au^- *Production in a Plasma-Sputter Type Negative Ion Source* ; Oct. 1991

NIFS-116 M. Sakamoto, K. N. Sato, Y. Ogawa, K. Kawahata, S. Hirokura, S. Okajima, K. Adati, Y. Hamada, S. Hidekuma, K. Ida, Y. Kawasumi, M. Kojima, K. Masai, S. Morita, H. Takahashi, Y. Taniguchi, K. Toi and T. Tsuzuki, *Fast Cooling Phenomena with Ice Pellet Injection in the JIPP T-IIU Tokamak;* Oct. 1991

NIFS-117 K. Itoh, H. Sanuki and S. -I. Itoh, *Fast Ion Loss and Radial Electric Field in Wendelstein VII-Λ Stellarator*; Oct. 1991

NIFS-118 Y. Kondoh and Y. Hosaka, *Kernel Optimum Nearly-analytical Discretization (KOND) Method Applied to Parabolic Equations <<KOND-P Scheme>>;* Nov. 1991

NIFS-119 T. Yabe and T. Ishikawa, *Two- and Three-Dimensional Simulation Code for Radiation-Hydrodynamics in ICF*; Nov. 1991

NIFS-120 S. Kawata, M. Shiromoto and T. Teramoto, *Density-Carrying Particle Method for Fluid* ; Nov. 1991

NIFS-121 T. Ishikawa, P. Y. Wang, K. Wakui and T. Yabe, *A Method for the High-speed Generation of Random Numbers with Arbitrary Distributions;* Nov. 1991

NIFS-122 K. Yamazaki, H. Kaneko, Y. Taniguchi, O. Motojima and LHD Design Group, *Status of LHD Control System Design* ; Dec. 1991

NIFS-123 Y. Kondoh, *Relaxed State of Energy in Incompressible Fluid and Incompressible MHD Fluid* ; Dec. 1991

NIFS-124 K. Ida, S. Hidekuma, M. Kojima, Y. Miura, S. Tsuji, K. Hoshino, M. Mori, N. Suzuki, T. Yamauchi and JFT-2M Group, *Edge Poloidal Rotation Profiles of H-Mode Plasmas in the JFT-2M Tokamak* ; Dec. 1991

NIFS-125 H. Sugama and M. Wakatani, *Statistical Analysis of Anomalous Transport in Resistive Interchange Turbulence* ;Dec. 1991

NIFS-126 K. Narihara, *A Steady State Tokamak Operation by Use of Magnetic Monopoles* ; Dec. 1991

NIFS-127 K. Itoh, S. -I. Itoh and A. Fukuyama, *Energy Transport in the Steady State Plasma Sustained by DC Helicity Current Drive* ;Jan. 1992